ICANS-XI International Collaboration on Advanced Neutron Sources
KEK, Tsukuba, October 22-26, 1990

Powder diffraction at ISIS

W I F David, S Hull, R M Ibberson and C C Wilson
ISIS Facility, Rutherford Appleton Laboratory, Chilton, Didcot, Oxon OX11 0QX, UK

ABSTRACT
The powder diffraction instruments at ISIS are described and examples given of the science performed.

I. INTRODUCTION

The field of powder diffraction at ISIS is well served by the availability of two powerful, complementary, high performance instruments. Both the High Resolution Powder Diffractometer HRPD and the Medium Resolution Powder Diffractometer POLARIS, are used in the performance of vigorous scientific programmes, some examples of which are given below.

II. HRPD – HIGH RESOLUTION POWDER DIFFRACTOMETER

The ISIS high resolution powder diffractometer HRPD (Figure 1) is the highest resolution neutron powder diffractometer in the world. Sitting at the end of a beam line almost 100m in length, and detecting in backscattering geometry, a resolution of $\Delta d/d \sim 5 \times 10^{-4}$ is achieved. Moreover, this resolution is essentially constant over the wide d-spacing range available (currently down to d-spacings of less than 0.3Å) making a much larger number of reflections available – and at higher resolution – than is possible on any other neutron powder instruments.

HRPD has dramatically extended the range of problems that can be tackled by powder diffraction. For example :

- Rietveld profile refinement of more complex structures are possible;
- Hydrogenous samples – often a problem for neutrons because of the high incoherent background – can be tackled;
- Crystal structures can be solved from powders *ab initio*;
- Structure refinements can be performed of a quality which previously required single crystals;
- The high resolution allows sophisticated peak shape analyses enabling the study of, for example, texture and strain.

II.1 Molecular structure of benzene

A fine example of the power of HRPD is given by recent work on benzene, C_6H_6 (David, 1989a). Benzene adopts an orthorhombic structure, space group Pbca ($Z=2$), with a moderately-sized unit cell ($a=7.3550$, $b=9.3709$, $c=6.6992$Å, $V=461.7$Å^3) (Figure 2). Although the original structure determination in 1928 located only the carbon atoms, the observed molecular planarity resolved a debate about whether the molecule was puckered, as favoured by a number of eminent scientists including Bragg, or flat.

Successive X-ray single crystal investigations improved the precision and accuracy of structure determination. The use of neutrons as a structural probe confirmed the planarity not only of the

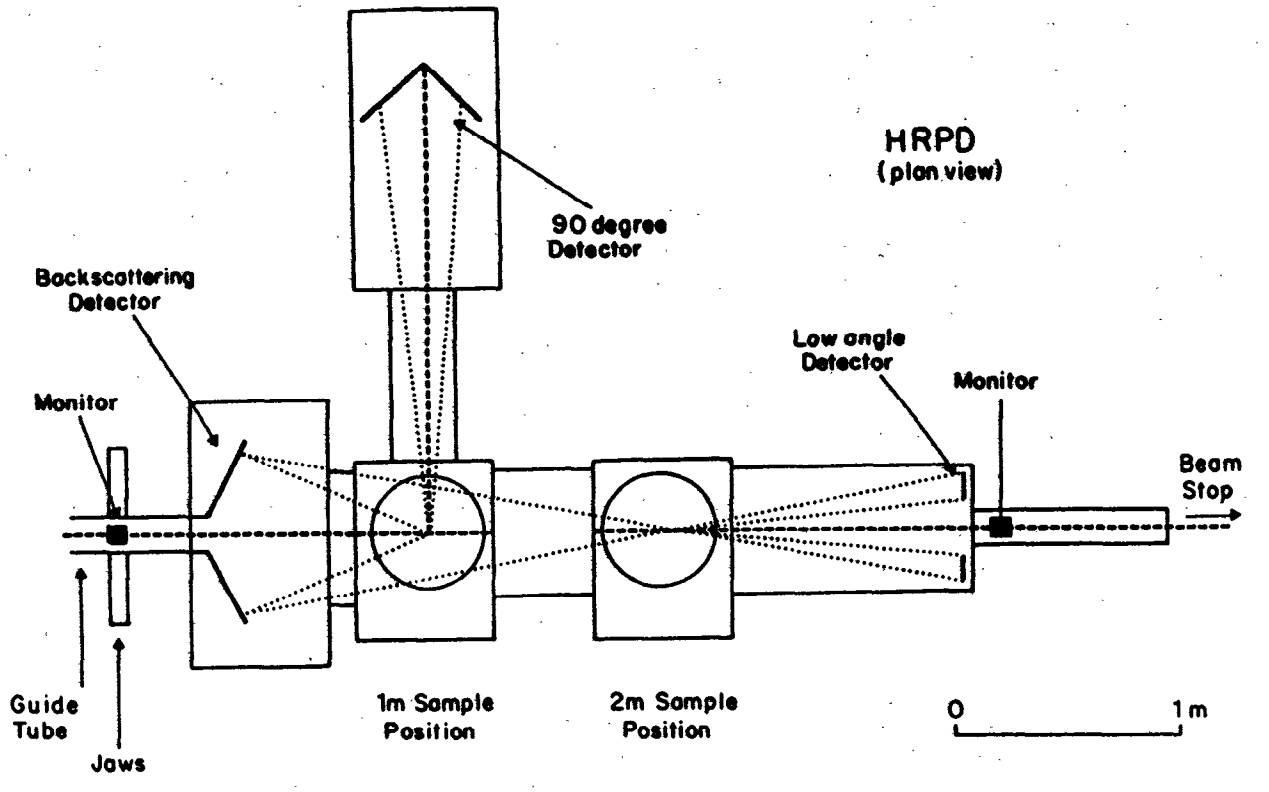

Figure 1 - Plan view of HRPD. The 2m sample position is some 96m from the moderator.

Figure 2 - The crystal structure of benzene.

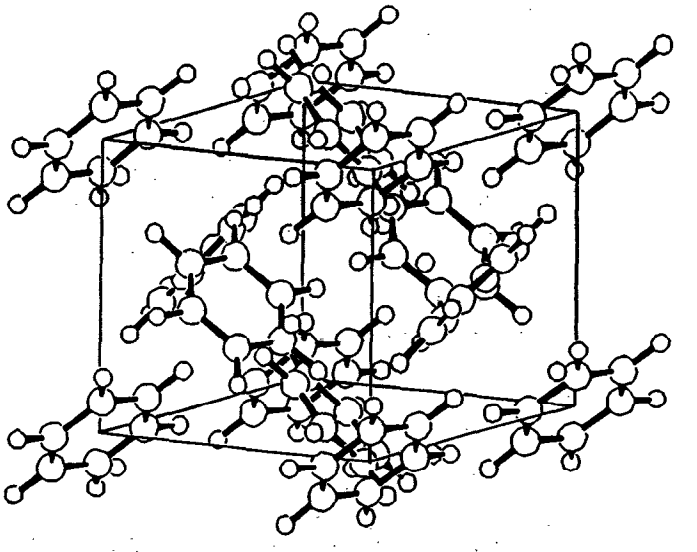

carbon but also the hydrogen atoms. A recent single crystal neutron diffraction investigation on deuterated benzene, C_6D_6 (Jeffrey, Ruble, McMullan and Pople, 1987), sought to investigate any deviations from planarity. In addition to contributing to continued investigations of the nature of the chemical bond, these experimental results have been compared with the latest theoretical calculations to assess the current status both of experimental technique and theoretical calculation. One further justification was given by Jeffrey for performing another single crystal neutron diffraction experiment: benzene "should be repeatedly investigated by each scientific method whenever there is a significant advance with respect to the detail or accuracy that the method can offer". It is therefore fitting that a detailed structural investigation of benzene be performed on HRPD to investigate (i) how well do the best powder diffraction experiments compare with equivalent single crystal studies for moderately complex structures with unit cells of the order of 500Å^3 and (ii) can reliable anisotropic temperature factors be obtained from time-of-flight powder diffraction experiments? The existence of both high precision single crystal data and detailed theoretical calculations provides a very rigorous test for the benzene data collected on HRPD.

Data were collected over a period of approximately nine hours (174 μA-hr). The raw data were corrected for incident flux (using a vanadium calibration), and cryostat and sample attenuation. The last correction was derived from consideration of the transmitted neutron flux and showed significant structure from multiple-scattering self-attenuation effects. Rietveld refinement was performed using the powder diffraction package developed at RAL and based upon the Cambridge Crystallography Subroutine Library. For data in the range 0.606-1.778Å an excellent least-squares fit to the powder diffraction data was obtained (Figure 3). The refined structural parameters included 18 atomic coordinates and 36 anisotropic temperature factors. With the exception of the B_{22} temperature factors for three carbon atoms, there is a remarkably good agreement between the positional and thermal parameters obtained from HRPD and from the single crystal data. More importantly, the anisotropic temperature factors for the deuterium atoms calculated using harmonic lattice dynamical calculations are significantly different from those obtained by both powder and single crystal diffraction techniques. Table 1 lists bond lengths, uncorrected for libration, obtained in the present study and from the work of Jeffrey et al (1987). The agreement is good, with few statistically significant differences, these probably resulting from systematic errors in the powder diffraction data.

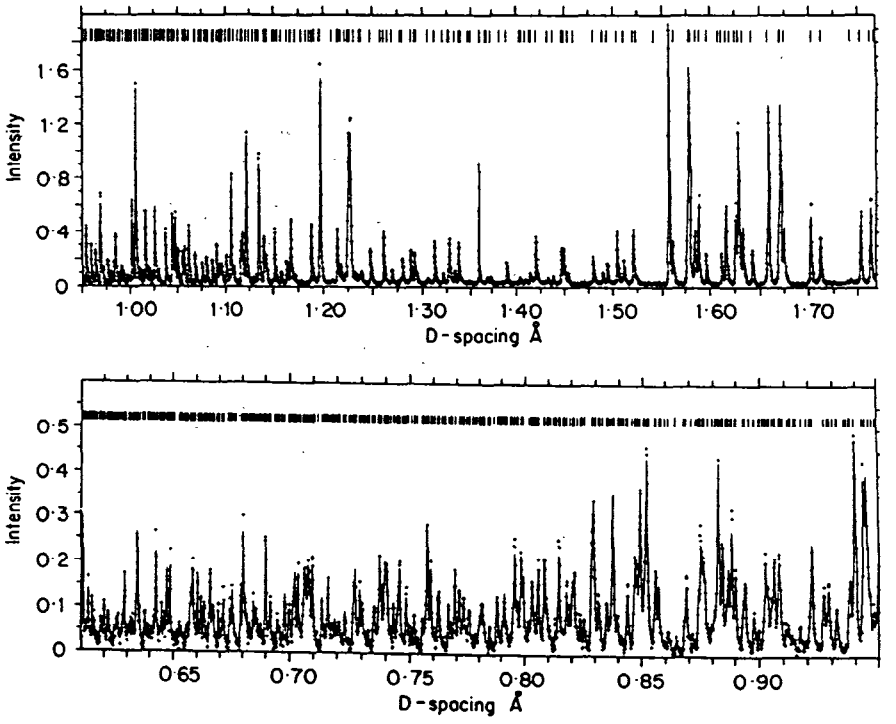

Figure 3 – The final profile fit of the HRPD low temperature benzene data, from which accurate anisotropic temperatures were obtained. The quality of fit is apparent.

TABLE 1 - Benzene : bond lengths in Å (uncorrected for libration)

HRPD data (5K)		Single crystal data (15K)	
C1-C2 = 1.3940(20)	C1-D1 = 1.0825(30)	C1-C2 = 1.3969(7)	C1-D1 = 1.0879(9)
C2-C3 = 1.4047(30)	C2-D2 = 1.0815(30)	C2-C3 = 1.3970(8)	C2-D2 = 1.0869(9)
C1-C3 = 1.3948(20)	C3-D3 = 1.0836(25)	C1-C3 = 1.3976(7)	C3-D3 = 1.0843(8)
mean = 1.3978(15)	mean = 1.0825(20)	mean = 1.3972(5)	mean = 1.0864(7)

At the present stage of analysis it is clear that the end results obtained from refinement of HRPD data are not significantly inferior to the best single crystal data. Both experimental techniques agree closely with each other, and differ from the theoretical calculations, particularly in the values obtained for the anisotropic temperature factors for the deuterium atoms. The powder diffraction experiment thus strongly supports the single crystal study and indicates that further improved theoretical calculations are required. The quality of these powder diffraction results represents present state of the art at ISIS. Further improvements in the normalisation procedure are currently under development and should lead to a precision and accuracy in moderately complex structure determination that is at least as good as the best single crystal results. This indeed represents a very significant advance in the power of powder diffraction.

II.2 Phase transition in Neopentylglycol

Neopentylglycol (NPG) is one of a series of substituted methane compounds of the type $C(CH_3)_4$-n(CH_2OH) (n = 0 to 4). NPG, corresponding to n = 2, exhibits a rigid to plastically-crystalline phase transition at 314.5 K common to all the series, but exhibits an additional low temperature phase transition at 60.4 K. The approximate molecular conformation was obtained (Suga, Matsuo and David, 1990) by a distance-least-squares refinement of atomic positions using a novel combination of chemical constraints. A total of 41 bond length and bond angle constraints define the molecule which when combined with limited single crystal X-ray data collected at room temperature can provide a good starting model for the solution attempt. From such a starting model the structures of the two low temperature phases were obtained using traditional constrained full profile refinement techniques. Both structures were found to be monoclinic, space group $P2_1/n$, with only a 0.2% change in the a, b and c lattice parameters and a 2% change in monoclinic angle, showing the transition to involve very subtle changes in hydrogen bonding. Such detailed knowledge is vital in understanding the inter- and intra-molecular forces which operate to produce the very large enthalpy of this transition, which gives the material potential technical applications as an energy storage material.

II.3 Peak Shape Effects - ferroelastic phase transition in $LaNbO_4$

Many of the diffraction patterns collected on HRPD show peak broadening effects that are dominated not by the instrument but by crystal imperfections within the sample. There is thus a need for a flexible description both of the peak shape function and peak width parameterisation. The final peak shape may be regarded as a multiple convolution of an instrumental resolution function and all the different sample dependent effects such as size, strain and stacking faults. Accordingly a peak shape algorithm based upon the convolution of individual components by fast Fourier transform techniques has been developed. This has the great advantage that, although the final peak shape function is complex, it may be obtained simply as the (inverse) Fourier transform of the product of the simple Fourier transforms of individual peak shape components. This has permitted the inclusion in the overall peak shape description of not only Gaussian and Lorentzian components but also truncated quadratic functions. A further important advance in the Rietveld analysis of HRPD data has been the development of a

program that permits the refinement of crystal structure parameters along with the Lorentzian and Gaussian components of each individual peak in the diffraction pattern. This results in a large number of parameters but has the advantage that one obtains peak widths that are unbiased by the imposition of an *hkl*-dependent peak broadening model. An example of the use of this technique is illustrated in the study of the material $LaNbO_4$.

Rietveld refinement of data collected from $LaNbO_4$ on HRPD at a number of different temperatures (David, 1989b) indicated that the anisotropic broadening resulted from strain rather than size effects (Figure 4). This anomalous behaviour is restricted to the ab plane: no extra broadening is associated with the c axis, with the refined values clearly indicating strain anisotropy within the ab plane.

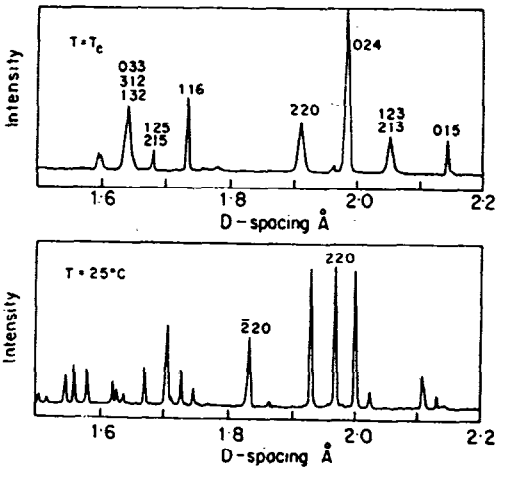

Figure 4 – The differences between diffraction patterns recorded at room temperature and T_c are extremely marked. Note the large anisotropy in peak widths at T_c, with (hk0) peaks being broad whereas predominantly c* reflections remain unaffected by the transition.

The anisotropic broadening of the Bragg peaks (microstrain) in $LaNbO_4$ may, as with the monoclinic lattice distortion (macrostrain), be described in terms of a second rank tensor. The principal axes of the ellipsoid representing the microstrain broadening is rotated by 21° from a*. This agrees to within experimental error (~ 2°) with the orientation of the principal axes of the spontaneous macrostrain hyperbola for all data sets collected between (T_c – 50°) and T_c. The coincidence of the orientation of microstrain (obtained from line broadening considerations) and macrostrain (calculated from peak splittings associated with monoclinic symmetry) was unexpected and is at present unexplained. It indicates, perhaps unsurprisingly, that unit cell and unit cell contents play a coherent role with respect to the phase transition. The importance of strain in the driving mechanism is associated with the fact that $LaNbO_4$ is a proper ferroelastic material – there is a soft acoustic mode but no observed soft optic mode. Further analysis of this phase transition using the structural information is currently underway.

The unexpected discovery of unusual strain broadening in $LaNbO_4$ and its implications for the phase transition mechanism highlights the advantages of high resolution. Although structure refinement involving the traditional Rietveld method is still the mainstay of neutron powder diffraction, there are a growing number of problems in materials science where high resolution has proved invaluable. The diversity of science tackled on HRPD confirms the success and assures the future of high resolution neutron powder diffraction.

III. POLARIS – MEDIUM RESOLUTION POWDER DIFFRACTOMETER

The medium resolution powder diffractometer POLARIS (Figure 5) is an instrument that is in many ways complementary to HRPD. Being situated considerably closer to the ISIS target, it sacrifices some resolution in favour of high count rates. POLARIS thus has the ability to study smaller or more weakly scattering samples. The loss of resolution is important, of course, especially when a material with a large, low symmetry unit cell, and hence many Bragg peaks in

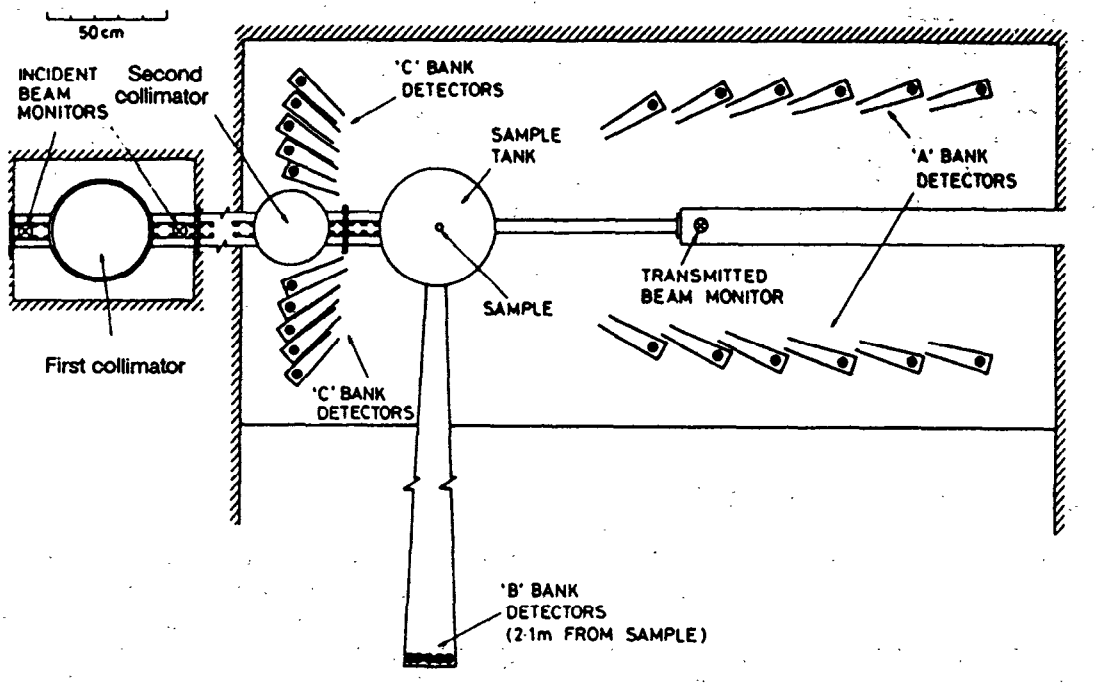

Figure 5 – Layout of POLARIS. The sample position is some 12m from the moderator.

the pattern, is being studied. To some extent, however, this problem is offset by the availability at ISIS of extremely powerful and flexible profile refinement packages.

In addition to having the capability to perform measurements on small samples over normal times, POLARIS also gives the possibility of taking data over very short times on samples of standard size. It is thus an appropriate instrument on which to look in real time at phase changes and solid state chemical reactions. Furthermore, the existence of a large detector bank at 90° allows high quality measurements on samples in pressure cells or other sample environment.

III.1 Measurements of Residual Stress

A knowledge of the residual stress distributions in engineering components is important for predicting their load carrying capabilities, failure characteristics and probable lifetimes. A test experiment has been performed on POLARIS to study the residual stress distribution within an autofrettaged steel ring (Webster and Webster, 1990). The sample was scanned through the beam, using a rig capable of remotely controlled x, y and z translations, together with an ω rotation about the vertical axis. A time-of-flight diffraction instrument, such as POLARIS, has the advantage of measuring the whole diffraction pattern from the individual 'pixels', which allows the lattice parameter a_0 to be obtained by least squares refinement over many reflections. The results are compared in Figure 6 with the values obtained using a fixed wavelength diffractometer at the ILL, where a_0 is determined from measurements of the (211) reflection alone. By measuring a large number of diffraction peaks in the same scattering direction POLARIS can provide additional information on the elastic anisotropy within the illuminated sample volume.

Figure 6 – A comparison between the residual strain measurements of an auto-frettaged ring on POLARIS (○) and D1A (●). Reasonable agreement is achieved except near the edges, probably a consequence of sample volume.

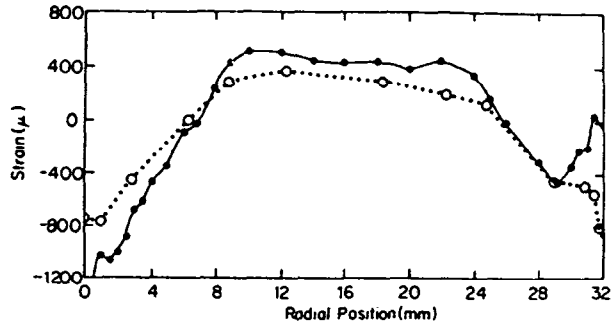

III.2 High pressure diffraction studies

Structural studies of powder samples under hydrostatic pressure are made difficult by the need to surround the sample by pressure transmitting components of the pressure cell. The fixed scattering geometry of a time-of-flight diffraction instrument allows collimation of the incident and scattered beams which eliminate spurious Bragg reflections from these components. One of the first successful experiments on samples under hydrostatic pressure on POLARIS, using the 'McWhan' clamped cell constructed at ISIS, is illustrated elsewhere (Hull, David, Ibberson and Wilson, this volume).

Figure 7 – Equation of state of LiD measured on POLARIS using the McWhan (●) and Paris (▪) pressure cells. The dashed line represents previous measurements. It can be seen that the POLARIS measurements differ appreciably from these, but agree very well with recent calculations (solid line).

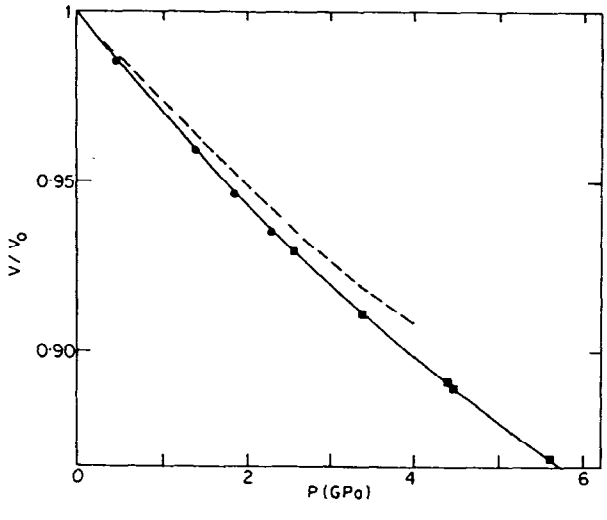

The collaborative project with the Universities of Paris and Edinburgh to develop a clamped cell for very high pressure neutron studies has also made significant progress, and is also detailed (Hull, David, Ibberson and Wilson, this volume). The equation of state of the quantum solid LiD has been measured to 70 kbar (Figure 7; Besson et al, 1991), the first time a sample volume of 100 mm3 has been studied above ~40 kbar. Future modifications, including the replacement of tungsten carbide anvils by sintered diamond, are now confidently expected to allow structural refinements to be performed in the pressure range above 100 kbar previously unexplored by neutrons.

III.3 Powder diffraction studies of the mechanism of battery discharge

Manganese dioxide, MnO_2, is widely used as the cathode material in alkaline batteries. Despite considerable research effort over the past 20 years, the processes which occur within the cathode of a cell during discharge are still not fully understood. In particular, it is unclear how the MnO_2 lattice accommodates protons during operation and how the structural behaviour is related to the ultimate failure of the cell. POLARIS has been used to obtain powder diffraction spectra of samples of MnO_2, taken from batteries at various stages of discharge (Figure 8; Clark, David and Hull, 1989).

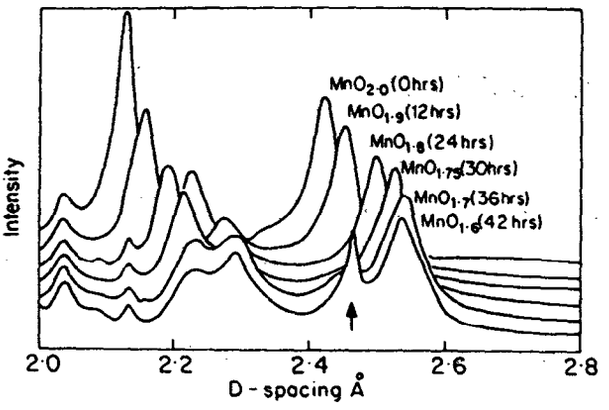

Figure 8 – Powder diffraction spectra taken from batteries at various stages of discharge. Indicated is the position of an additional Bragg peak, attributed to the formation of an ordered Mn–O–H phase. The appearance of this phase coincides closely with the point of battery failure.

Structural investigations of MnO_2 are made difficult by the poorly crystalline nature of the samples and the many, essentially similar, allotropic forms adopted by MnO_2, which comprise different arrangements of MnO_6 octahedra. Simulations of the powder diffraction spectra have been performed, using the known structures of the most common crystalline forms, pyrolusite (single chains of edge-sharing MnO_6 octahedra) and ramsdellite (alternating double chains of linked MnO_6 octahedra). These are found to differ significantly from the diffraction pattern measured from the MnO_2 in its undischarged state. It is possible, therefore, to discount these structures, plus that of γ–MnO_2, which comprises an irregular intergrowth of pyrolusite and ramsdellite layers. Surprisingly, adequate agreement is achieved by adopting the little known ϵ–MnO_2 structure, with hexagonal close packed O^{2-} ions and half the octahedral sites occupied by Mn^{4+}.

It is clear from Figure 8 that significant structural changes occur during battery discharge, including the expansion of the lattice associated with the intercalation of protons. These results give the first direct experimental evidence of proton insertion into MnO_2. Preliminary analysis suggests that the protons are accommodated randomly within the remaining empty octahedra in the ϵ–MnO_2 lattice. There is also evidence of additional broad diffraction peaks which appear after about 36 hours discharge. This coincides closely with the point of battery failure. These extra Bragg peaks are attributable to the formation of ordered Mn–O–H phases which essentially hinder proton diffusion through the MnO_2 lattice.

References

Besson J M, Weill G, Nelmes R J, Loveday J S and Hull S, High Pressure Research, submitted (1991)

Clark J W, David W I F and Hull S, ISIS 1989 Annual Report, RAL–89–050, 68 (1989)

David W I F, ISIS 1989 Annual Report, RAL–89–050, 43 (1989a)

David W I F, ISIS 1989 Annual Report, RAL–89–050, 47 (1989b)

Jeffrey G A, Ruble J R, McMullan R K and Pople J A, Proc. Roy. Soc. Lond. A414, 47 (1987)

Suga H, Matsuo T and David W I F, ISIS 1990 Annual Report, RAL–90–050, A31 (1990)

Webster G A and Webster P J, ISIS 1990 Annual Report, RAL–90–050, A63 (1990)